Enhanced S-band fiber laser performance with a thulium-doped ZBLAN photonic crystal fiber

A. R. MUHAMMAD[a], H. AHMAD[a], S. W. HARUN[a,b]
[a]*Photonics Research Centre, University of Malaya 50603 Kuala Lumpur, Malaysia*
[b]*Department of Electrical Engineering, University of Malaya, 50603 Kuala Lumpur, Malaysia*

A new method is proposed and studied to improve the lasing performance of a Thulium-doped fiber laser (TDFL) using a photonic crystal fiber (PCF) filter approach. Fluoride, ZBLAN was used as the host material for the proposed PCF gain medium with an amplified spontaneous emission (ASE) suppression capability. The PCF was designed by using finite element method (FEM) analysis to suppress both Thulium's ASEs at 0.8 µm and 1.8 µm band and thus increases the population inversion in S-band region. S-band lasing enhancements on slope efficiency was observed to improve from 65% to 73% when compared with normal TDF at the wavelength region between 1.42 and 1.47 µm.

(Received July 14, 2014; accepted September 11, 2014)

Keywords: Photonic crystal fiber (PCF), Thulium, filter based fiber, ASE suppressions

1. Introduction

Due to tremendous increase in communication traffic in recent years, Thulium-doped fiber amplifiers (TDFAs) become a promising candidate especially for amplification in S-band region. In spite of advantages of TDFA in amplification at S-band region, there are some of the spectroscopic challenges that affect the S-band amplification [1]. Longer lifetime of the lower amplifying level than upper level, amplified spontaneous emissions (ASEs) from upper level (0.8 µm) and competing transitions in other regions are some factors that reduce the gain in S-band region. Thulium doped fiber (TDF) with silica host is a candidate that produce high phonon energy and leads to the very short $^3H_4$ radiative lifetime [2].

In this paper, we present a new method to improve gain and lasing characteristics of fluoride or ZBLAN based TDF in the S-band region by suppressing both ASE generations at 0.8 µm, and 1.8 µm bands. In the proposed simulation, Full-Vectorial Finite Element Method (FV-FEM) simulation was used to design a photonic crystal fiber (PCF), which has core doped with Thulium ion and the structure has a desired filtering characteristic that allows the suppression of both 0.8 µm, and 1.8 µm ASEs. This micro-structured optical fiber with periodic arrangement of low index material in a background of high refractive index is optimized to achieve a band-pass filter to suppress the unwanted ASE. This causes a higher emission at 1.4 µm that eventually lead to higher stimulated emission and better S-band amplification.

2. Spectroscopy characteristic of Thulium doped fiber

In order to design an efficient Thulium-doped fiber lasers (TDFLs), it is necessary to understand the spectroscopic properties of the TDF. There are a few challenges regarding the spectroscopic properties of this fiber that affects the S-band lasing. The host dependent issue regarding the domination of non-radiative decay from the upper and lower amplification level and self-terminating ion transition due to the longer lifetime at lower laser level compared to upper level are two main spectroscopic challenges in designing S-band TDFL [3]. The other obstacles especially when employing the fiber for generating S-band laser is its competing transition in other regions namely at 0.8 µm and 1.8 µm [4]. Therefore, in this work, we design a filter based fiber that can suppress these unwanted amplified spontaneous emission (ASEs) bands together with the employment of low phonon energy glass, fluoride type fiber namely ZBLAN as the host material of the fiber to improve the laser performance of the TDFL at S-band region.

Fig. 1 shows the emission and absorption spectra of a TDF with a ZBLAN host. Here, we numerically simulate the TDFL by utilizing the emission and absorption spectra properties of TDF at 0.8 µm, 1.4 µm and 1.8 µm bands. Radiative lifetimes for ZBLAN host was taken into account as they are one of the primary factors that influence the S-band emission. It is reported that by using ZBLAN fiber the fluorescence lifetime can be improved from 14.2 µs to 1350 µs when compared with pure silica fiber [5-7]. The spectral emission cross-section of thulium ion as in [8] can be estimated from the spectral absorption cross-section by the modified McCumber's relation [9]. Based on the experimental observation, it was found that the absorption cross section peak is approximately 70% of the emission peak.

According to Fig. 1, both emission at 0.8 µm and 1.8 µm are higher than the intended region at 1.4 µm. Hence, the need to suppress the 0.8 and 1.8 µm ASE becomes crucial in order to allow stronger emission at 1400 nm and producing a high S-band emission. Here, we use photonic crystal fiber (PCF), which is doped with a Thulium ions as the gain medium. The PCF is also designed to suppress both 0.8 µm and 1.8 µm ASEs and thus allows an efficient laser generation in S-band region.

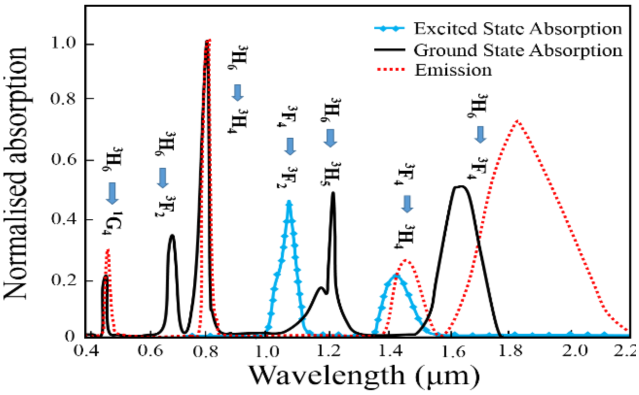

Fig 1. The emission and absorption spectra of the TDF.

3. Designing PCF filter

PCF is an attractive technology of fiber that can leads to a numerous difference application based on their geometrical structures. One of the unique properties of PCF is that its transmission windows or band-pass filtering characteristic can be controlled by manipulating the geometry structure. In order to realize the desired PCF filter, we deploy the strategies reported by Varshney [10]. Fig. 2(a) shows the cross section view of the proposed PCF, which have four important geometrical properties; lattice constant Λ, core diameter *D* (Λ = *D*), first ring air holes diameter *d'* that surrounding the core, and cladding air holes diameter *d*. By controlling the diameter of *d*', the long cut-off wavelength of the fiber can be adjusted. This cut-off point was determined by using the mechanism of intersection point value between the fundamental modes n_{eff} and cladding mode index n_{cl}. Fig. 2 (b) shows the simulation result of high and low cut-off wavelengths as a function of *d'* and *d*. In the simulation, *d*' is varied from 0.70 to 2.70 µm while d is changed from 0.8 until 1.28 µm with increment of 0.16 µm. The Λ = *D* is fixed at 3.2 µm. To control the short cut-off wavelength, doping the cladding region with high index material was suggested. The core-cladding index difference is defined by $\Delta = n_{core} - n_{cladding}$. Based on our criteria, Δ = -0.003 was chosen as it yield to a desired transmission spectra characteristic [10]. The shaded region of Fig. 2 (b) shows a set of cut-off wavelength together with *d* and *d'* value. It is found that the low loss transmission within 1 µm to 1.75 µm region can be realized by choosing *d* =0.96 and *d'*=1.185 µm according to our criteria.

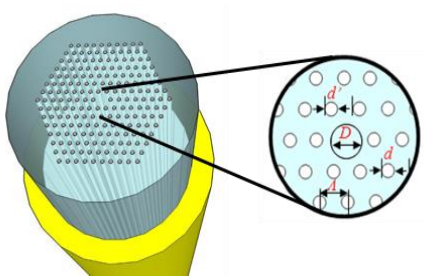

(a)

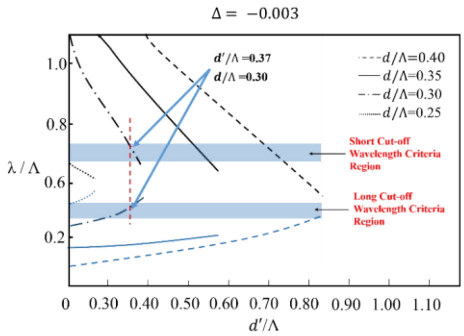

(b)

Fig. 2. (a) Geometrical structure of PCF (cross section view) and (b) long and short cut-off wavelengthsas a function of d' and d.

4. Laser configuration and energy level diagram of Thulium ion

Fig. 3 shows the configuration of the proposed TDFL, which consists of a PCF based ZBLAN TDF, a WDM coupler, a pump laser and two optical mirrors. The TDF length is fixed at the optimum value of 19 m. The 1.05 µm pump light and the input signal are combined using the WDM coupler and the laser power is coupled out from the output mirror. Two optical mirrors operating at 1.47 µm region with different reflectivities of 98% and 20% were used. This mirrors provides laser cavity in which allow laser radiation to pass and circulate the gain medium thus leads to a lasing output once it reached their threshold point. The output laser is tapped out from a 20% mirror port and measured by using optical spectrum analyzer (OSA) and power meter (PM).

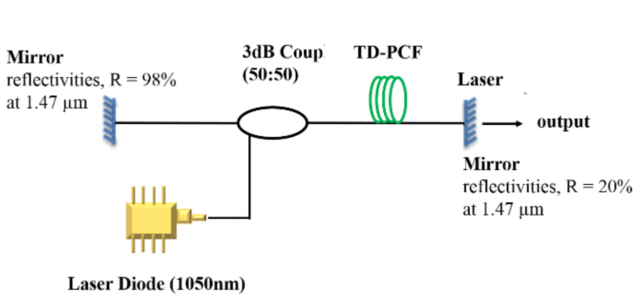

Fig. 3. Configuration of TD-PCF laser.

Figs. 4(a) and 4(b) show the absorption and emission transitions of trivalent thulium ions in glass, respectively with 1.05 µm pumping. As shown in the figure, the main transition used for S-band amplification is between $^3H_4$ and $^3F_4$ levels, which emit photons at 1.46 µm region. This amplification is made possible by an up-conversion pumping method, which forms a population inversion between $^3H_4$ and $^3F_4$ levels. When the TDF is pumped with 1.05 µm laser, the ground state ions in the $^3H_6$ energy level can be excited to the $^3H_5$ energy level and then relaxed to the $^3F_4$ energy level by non-radiative decay. The $^3F_4$ energy level ions are then re-excited to the $^3F_2$ energy level and experience non-radiative decay to the $^3H_4$ energy level via excited state absorption. This shows that 1.05 µm pump alone can provide both the ground-state and excited-state absorptions [4].

The difference between the $^3F_2$ and $^3F_3$ energy levels is very small and therefore they can be treated as one level for simplicity. We substitute N_0, N_1, N_2, N_3, N_4 and N_5 variables for ion populations of $^3H_6$, $^3F_4$, $^3H_5$, $^3H_4$, $^3F_2$ and $^1G_2$ respectively.

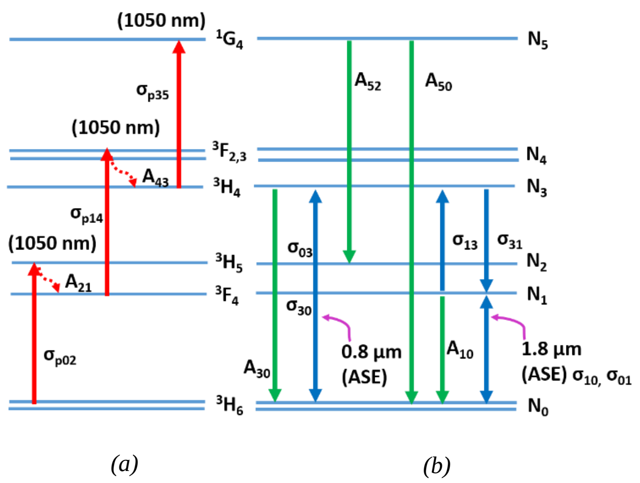

Fig. 4. Energy level diagram of thulium ion showing the (a) absorption transitions and (b) emission transitions.

According to Fig. 4(a) and (b) the rate equations can be established as follows [11];

$$\frac{dN_0}{dt} = -(W_{p02} + W_{18a} + W_{8a})N_0 + (A_{10} + W_{18e})N_1 + (A_{30} + W_{8e})N_3 + A_{50}N_5 \tag{1}$$

$$\frac{dN_1}{dt} = (W_{18a})N_0 - (A_{10} + W_{p14} + W_{sa} + W_{18e})N_1 + (A_{20})N_2 + (W_{se})N_3 \tag{2}$$

$$\frac{dN_2}{dt} = (W_{p02})N_0 - (A_{21}{}^{nr})N_2 + (W_{52})N_5 \tag{3}$$

$$\frac{dN_3}{dt} = (W_{8a})N_0 + (W_{sa})N_1 - (A_{30} + W_{p35} + W_{se} + W_{8a})N_3 + (A_{43})N_4 \tag{4}$$

$$\frac{dN_4}{dt} = (W_{p14})N_1 - (A_{43}{}^{nr})N_4 \tag{5}$$

$$\frac{dN_5}{dt} = (W_{p35})N_3 - (A_{50} + A_{52})N_5 \tag{6}$$

$$\sum_i N_i = \rho \tag{7}$$

The lasing performance of the proposed TD-PCF laser is simulated based on the above rate equations.

5. Result and discussion

The filtering characteristic of the PCF is strongly determined by the loss spectrum of the fiber and the overlap factor ($\Gamma(\lambda)$). The overlap factor is a measure of the portion of the optical mode which overlaps with the doped ion at the central core distribution that will stimulate absorption or emission from rare earth ion transitions. Fig. 5(a) shows the simulated overlap factor spectrum, Γ (λ) of the proposed TD-PCF at the optimized parameter settings of D = 3.2 µm, d = 0.96 µm and d' = 1.185 µm. As shown in the spectrum, the overlap between optical modes and dopants ions at wavelengths shorter than the first cut-off wavelength is very low, which is in good agreement with the electric field intensity analysis. At this wavelength region, the cladding modes is dominant where the optical field propagates inside the cladding instead of central core. This is due to cladding effective index is higher than effective index of fundamental mode at this wavelength region [10]. At the operating wavelength exceeds the first cut-off wavelength, the overlap factor value increased sharply due to the optical mode field is guided inside the core and thus more optical mode will overlap with the doping ions. This effect can be manipulated to control the optical gain spectrum of the TD-PCF

Fig. 5(b) shows the simulated gain as a function of TDF length for both standard TDF and TD-PCF, which was designed to suppress ASE in both 0.8 μm, 1.8 μm bands. The input signal wavelength and power are fixed at 1.46 μm and -30 dBm respectively, while the 1.05 μm pump power is fixed at 350 mW. Due to higher signal and pump overlap factor in the TD-PCF rather than the normal TDF, higher amount of pump power was depleted so the optimized fiber length is higher in the proposed TD-PCF compared to the standard TDF.

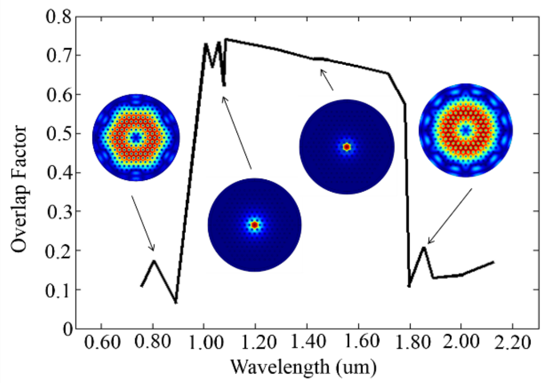

(a)

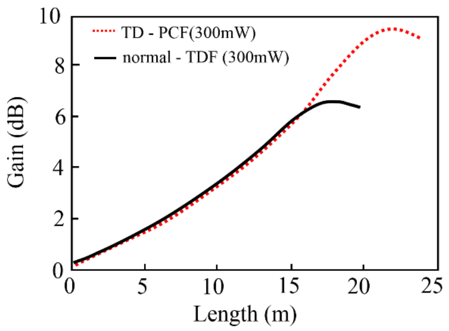

(b)

Fig. 5. (a) PCF Overlap factor curve for TD-PCF. (b) Gain as a function of position in the normal TDFA and TD-PCFA.

Figs. 6 (a) and (b) show the forward and backward ASE intensities against the cavity length for both TDF and TD-PCF lasers, respectively. This two categorized figure brings the information about the forward and backward 1.47 μm ASE travelling that indicated by blue and red lines respectively. The calculated optimum cavity length is obtained at 19 m. By comparing both figures, it is obtained that the TD-PCF produces a great increment on output power from 42 mW to 55 mW. This ASR enhancement reveals that by suppressing the unwanted ASE in thulium emission namely below 0.8 μm and above 1.8 μm, we can shift the emission towards the intended region, 1470 nm as in our case. Fig. 7 shows the output power curve of the laser against the pump power for both normal TDF and TD-PCF ZBLAN host media. It is observed that the slope efficiency of the proposed TD-PCF laser is up to 73%, which is about 8% better than the normal TDFL. Furthermore, both lasers configured with the normal TDF and PCF type have a threshold pump power of 185 mW and 164.4 mW, respectively. This reveals that the proposed TD-PCF laser has a lower pumping threshold as well as provides a better lasing efficiency.

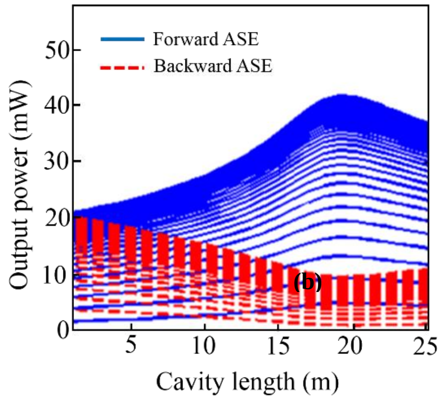

(a)

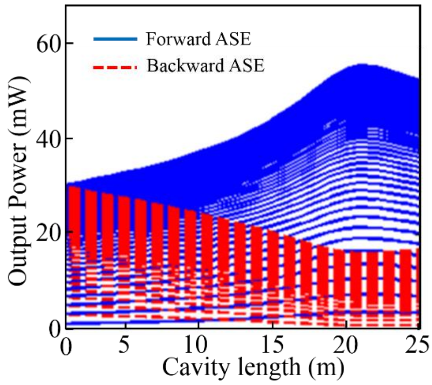

(b)

Fig. 6. ASE output power of ZBLAN host fiber for (a) normal TDF and (b) TD-PCF.

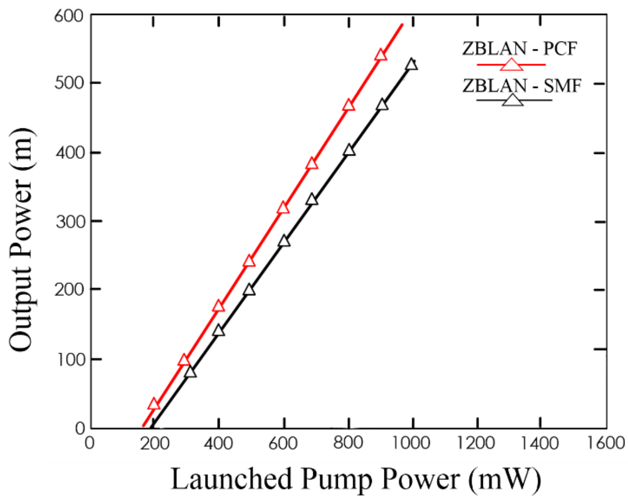

Fig. 7. Output power characteristic as function of pump power.

6. Conclusion

The optimized design of TD-PCF is demonstrated theoretically. The performance of the fluoride or ZBLAN based TDFL is better than the conventional TDFL with a normal SMF TDF as the gain medium. The TD-PCF was designed so that the wavelength higher than 1 μm propagates with low loss and high overlap factor in order to maximize the efficiency of the proposed TDFL with 1.05 μm pumping. Thulium absorption overlap factor is adjusted through PCF to allow the fundamental mode of the S-band signal to propagate with zero loss and high overlap factor while 0.8 μm and 1.8 μm ASE encounters higher loss and low overlap. In order to achieve above criteria, the optimize PCF geometrical structure is found at Λ = 3.2 μm, d'/Λ = 0.35, d/Λ = 0.30, and Δ = -0.003. It is found that S-band lasing performance shows a significant improvement when using ZBLAN based fiber on thulium PCF design. In conclusion the S-band lasing improves as we employed this filter-based fiber.

Acknowledgement

This work was supported by funding from the University of Malaya Research Grant Scheme (Grant No.: RP008C-13AET and PG139-2012B)

References

[1] T. Sakamoto, S. Aozasa, M. Yamada, M. Shimizu, Journal of Lightwave Technology, **24**, 2287 (2006).
[2] B. Faure, W. Blanc, B. Dussardier, G. Monnom, P. Peterka, 2004, p. OWC2.
[3] B. Faure, W. Blanc, B. Dussardier, G. Monnom, Journal of Non-Crystalline Solids, **353**, 2767 (2007).
[4] T. Kasamatsu, Y. Yano, T. Ono, Lightwave Technology, Journal of, **20**, 1826 (2002).
[5] P. Peterka, I. Kasik, V. Matejec, W. Blanc, B. Faure, B. Dussardier, Optical Materials, **30**, 174 (2007).
[6] W. Blanc, P. Peterka, B. Faure, B. Dussardier, G. Monnom, I. Kasik, Photonics, Devices, and Systems III, **6180**, V1800 (2006).
[7] S. D. Jackson, T. A. King, Journal of Lightwave Technology, **17**, 948 (1999).
[8] J. F. D. Michel, Rare-Earth-Doped Fiber Lasers and Amplifiers, Revised and Expanded, ed: CRC Press, 2001.
[9] E. Desurvire, ed New York: John Wiley & Sons, 1994.
[10] S. K. Varshney, K. Saitoh, N. Saitoh, Y. Tsuchida, M. Koshiba, R. K. Sinha, Optics Express, **16**, 9459-9467 (2008).
[11] S. Aozasa, T. Sakamoto, T. Kanamori, K. Hoshino, K. Kobayashi, M. Shimizu, IEEE Photonics Technology Letters, **12**, 1331 (2000).

*Corresponding author: swharun@um.edu.my